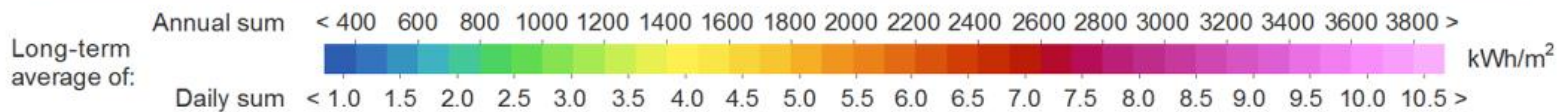
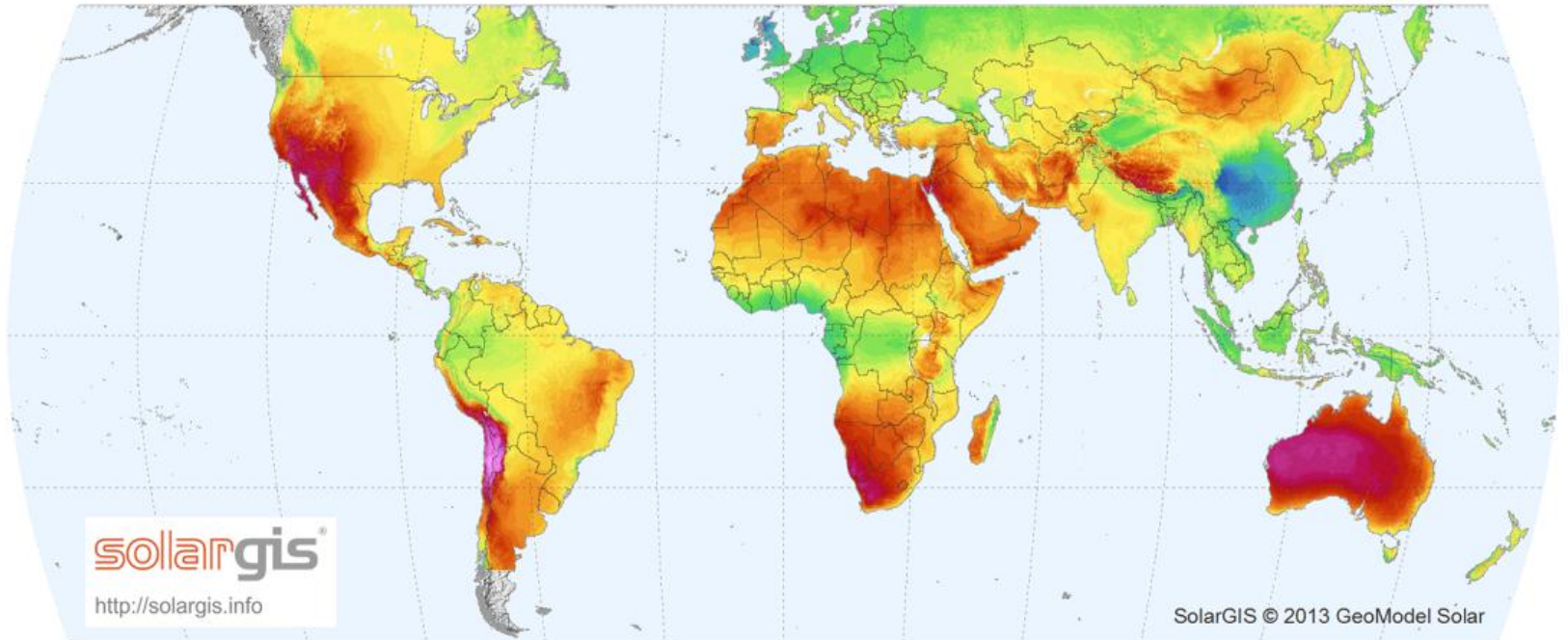


Background

WORLD MAP OF DIRECT NORMAL IRRADIATION

GeoModel
SOLAR



Long-term average of direct normal solar irradiance on a world map showing the potential of solar power generation in southern Africa (GeoModel Solar, 2014)

*South Africa has one of the **best solar resources in the world** and this resource is free to use and study for all South Africans, who should take the lead in this field in terms of*

- *skills development,*
- *training and*
- *product manufacturing.*

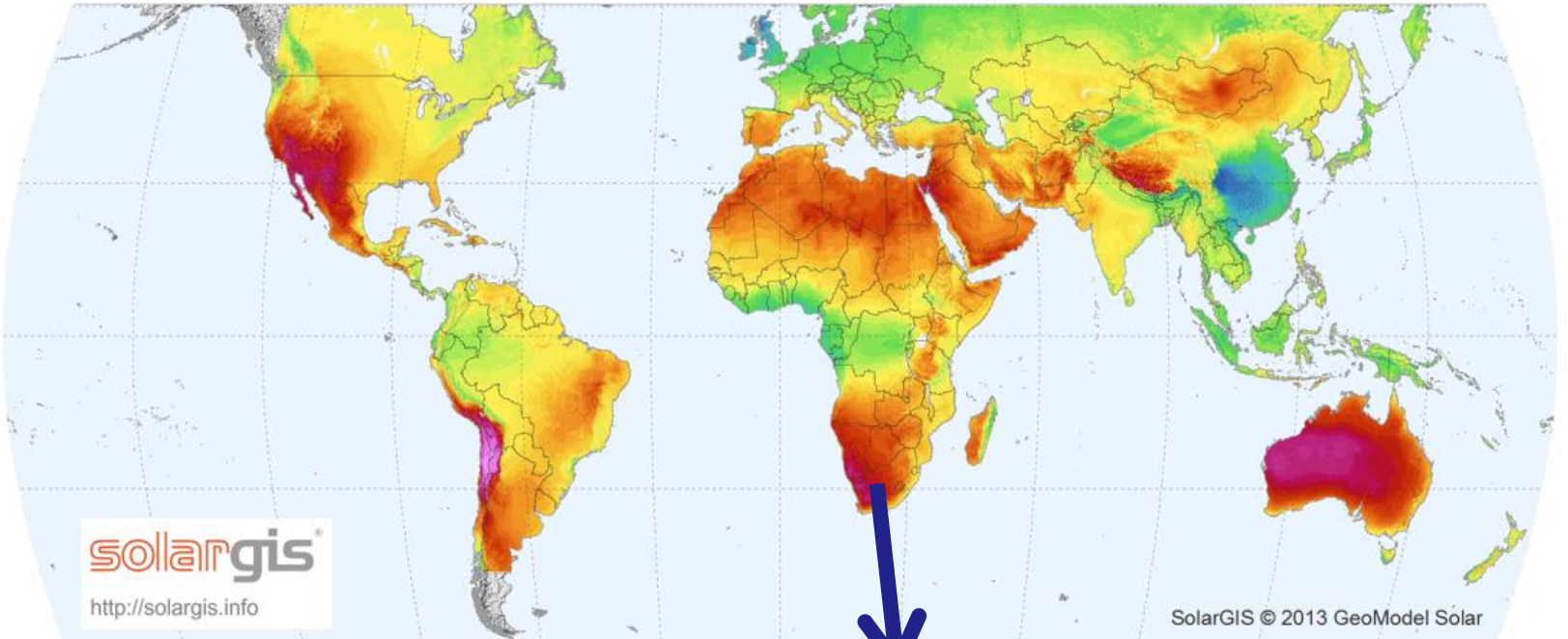
The research and development of solar dish technologies is a new and exciting research field in which all South African researchers of all age, race and gender can take the lead.



Background

WORLD MAP OF DIRECT NORMAL IRRADIATION

GeoModel
SOLAR



solarGIS

<http://solargis.info>

SolarGIS © 2013 GeoModel Solar

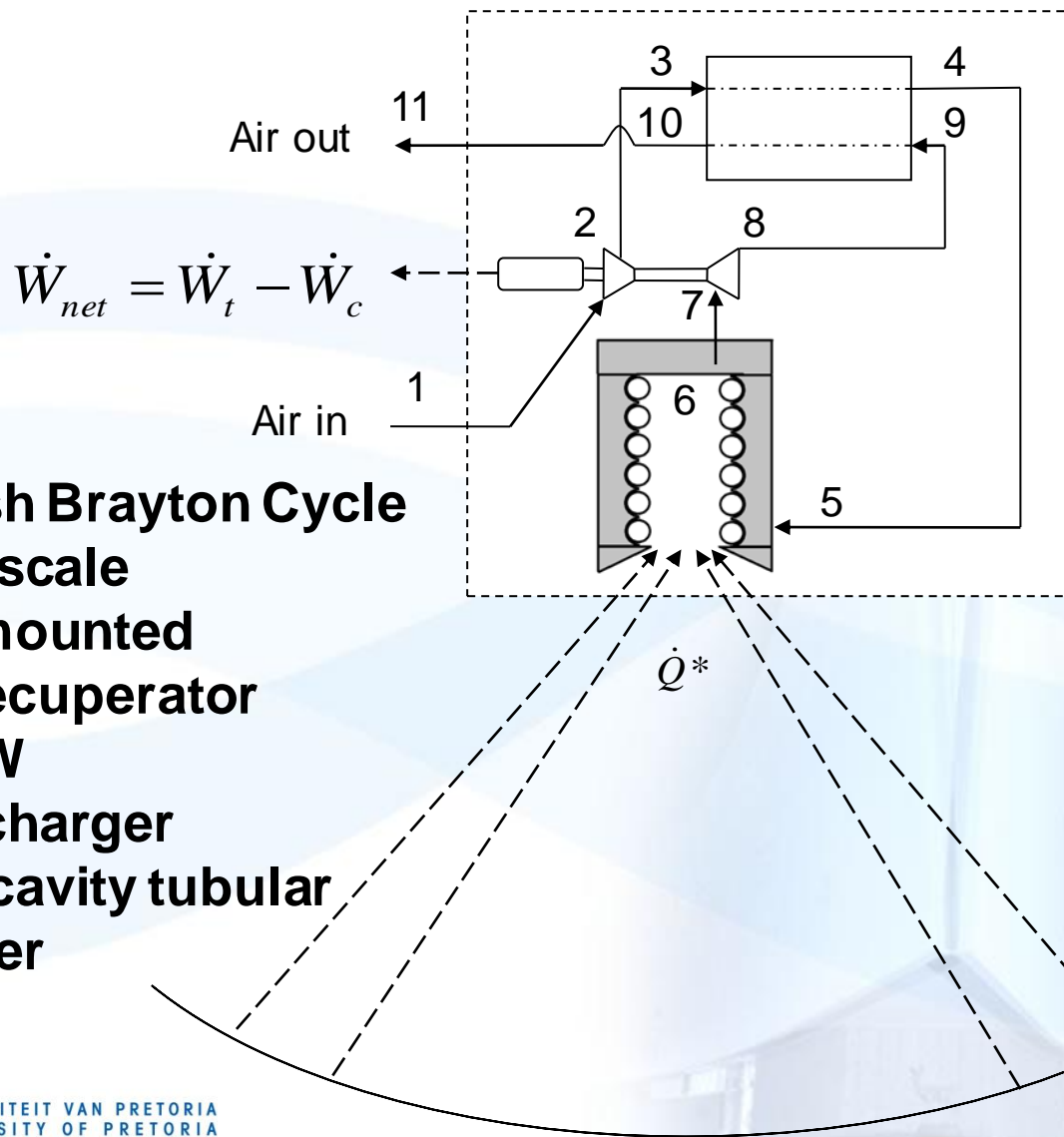
1. Power generation
2. Water purification
3. Fuel production



Presentation Outline

1. Introduction and Background
2. Problem and Purpose
3. Methodology
4. Results and Discussion
5. Conclusion
6. Progress to date (Solar@UP)
 - Solar radiation in Pta
 - New dish concept
 - Moonlight testing
 - Receiver testing
 - Recuperator testing

1. Introduction

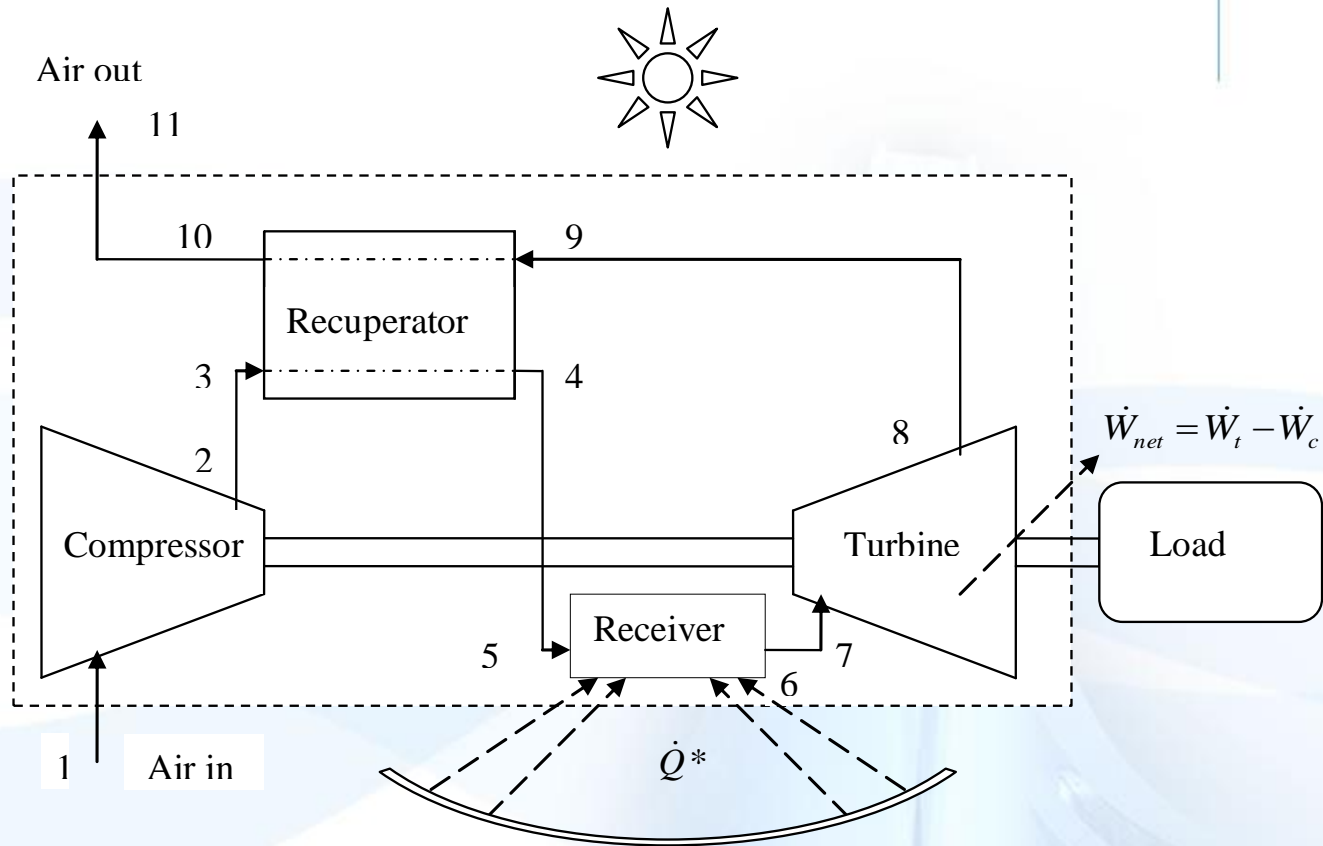


Proposed turbocharger to use as micro-turbine
(Image extracted from Garrett, 2014)

Solar-Dish Brayton Cycle

- small-scale
- dish-mounted
- with recuperator
- 1-20kW
- turbocharger
- open-cavity tubular receiver

1. Introduction

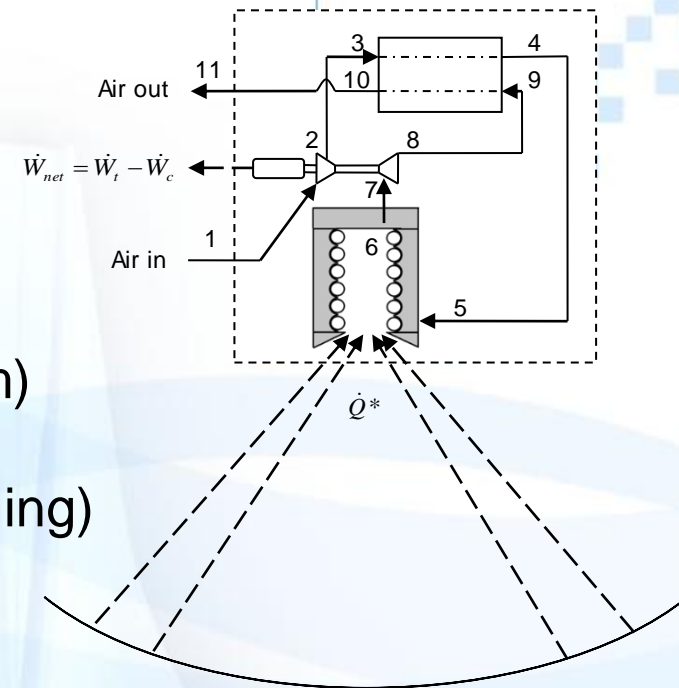


The small-scale dish-mounted solar thermal Brayton cycle with recuperator (STBC)

1. Introduction

Solar thermal Brayton cycle advantages

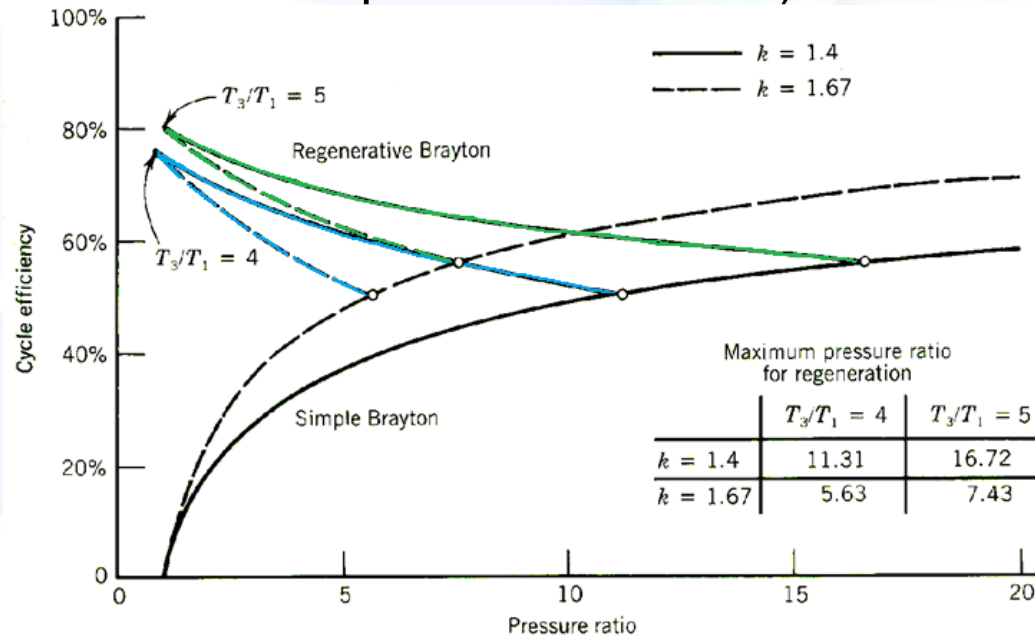
- Air as working fluid
 - Turbocharger as micro-turbine
 - Can also be powered with gas (hybrid system)
 - Water heating (cogeneration)
 - High efficiency potential (reheat and intercooling)
 - Mobility
 - Cost benefits (bulk manufacturing)
 - Thermal storage
-
- Quicker to commercialise (prototyping is quicker and cheaper)
 - Large-scale local manufacturing – good for the economy (good for South Africa)
 - Micro-grids



1. Introduction

Solar thermal Brayton cycle advantages

- **Recuperator**
 - allows for higher efficiency at lower compressor pressure ratios
 - allows for a less complex receiver (operating at lower pressure and smaller temperature increase)



1. Introduction

Solar thermal Brayton cycle advantages

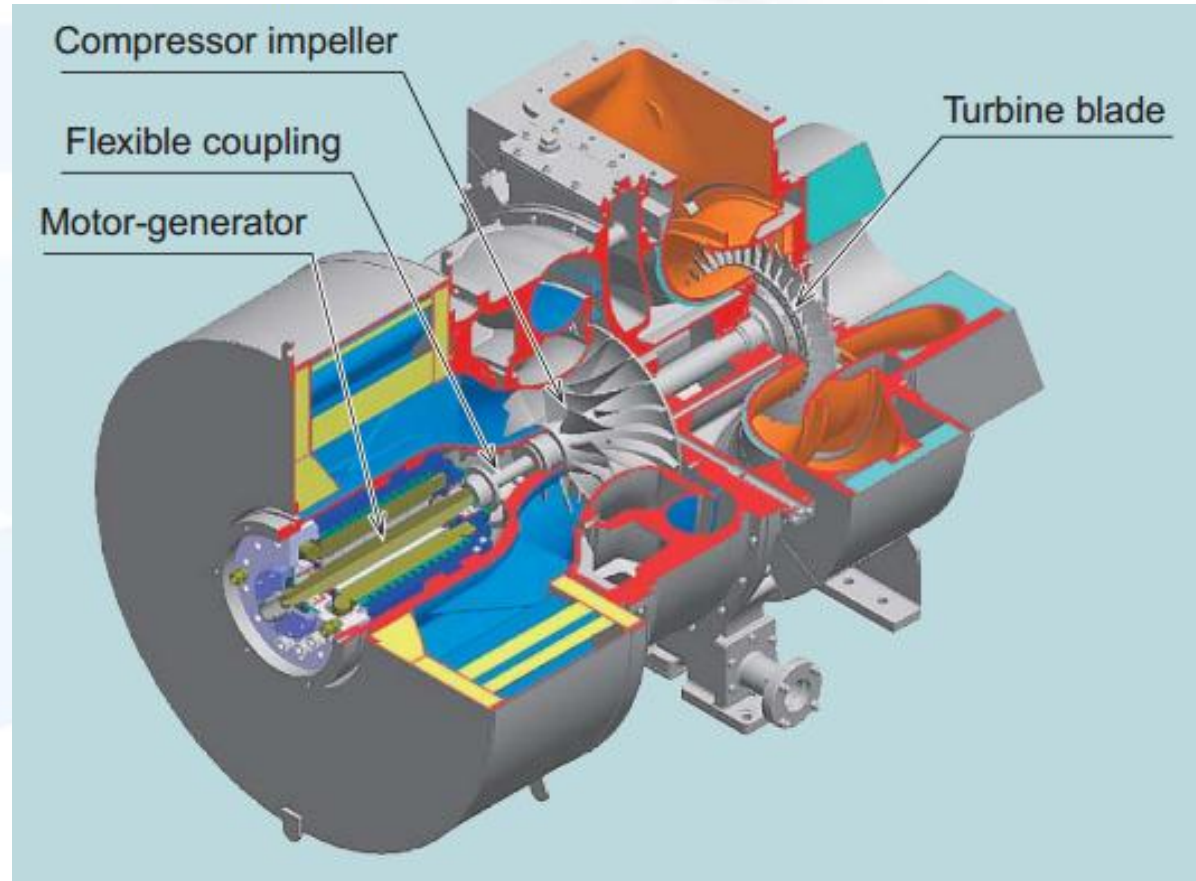
- **Turbocharger**
 - The maximum inlet temperature of an off-the-shelf turbocharger is about 1223 K (Garrett, 2014; Shah, 2005) and 1323 K intermittently.



**Proposed turbocharger
to use as micro-turbine**
(Image extracted from Garrett, 2014)

1. Introduction

- Turbocharger
 - Generator coupling



**Range extenders
in electric
vehicles**

1. Introduction

- Turbocharger
 - Generator coupling



**Generator coupling – simple, robust, easy to maintain
(Image extracted from Shiraishi and Ono, 2007)**



1. Introduction – Open cavity tubular receiver

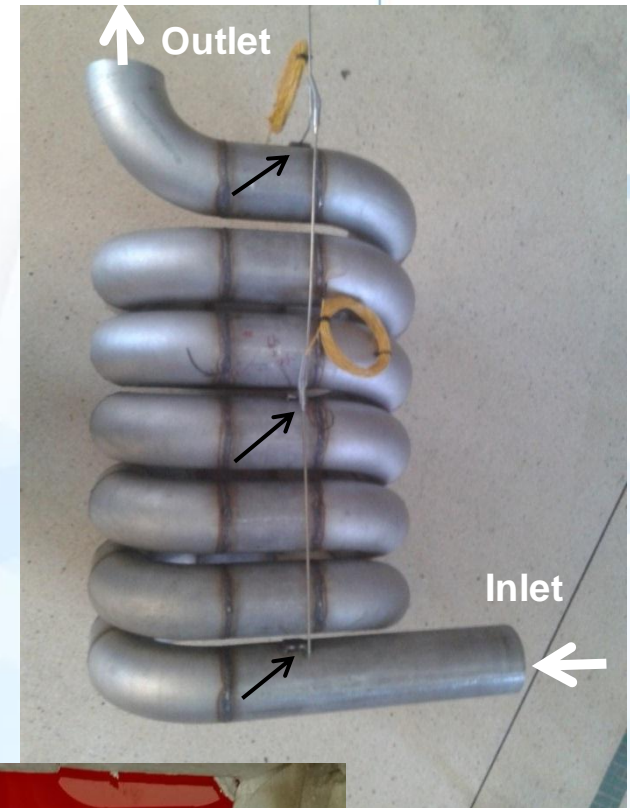
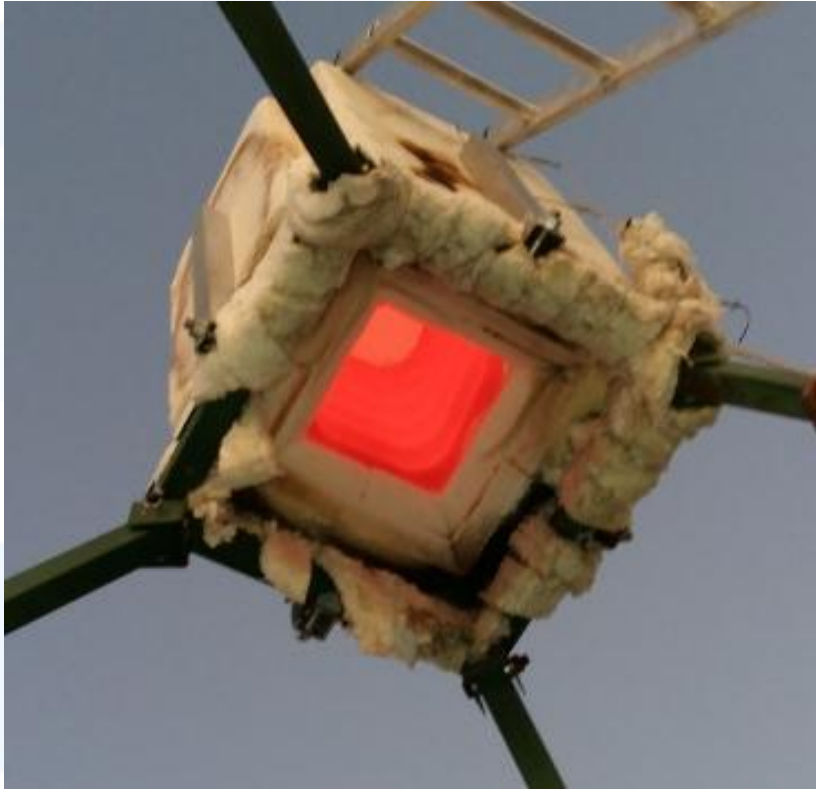


Receiver dimensions optimised in a previous work (Le Roux et al., 2014)

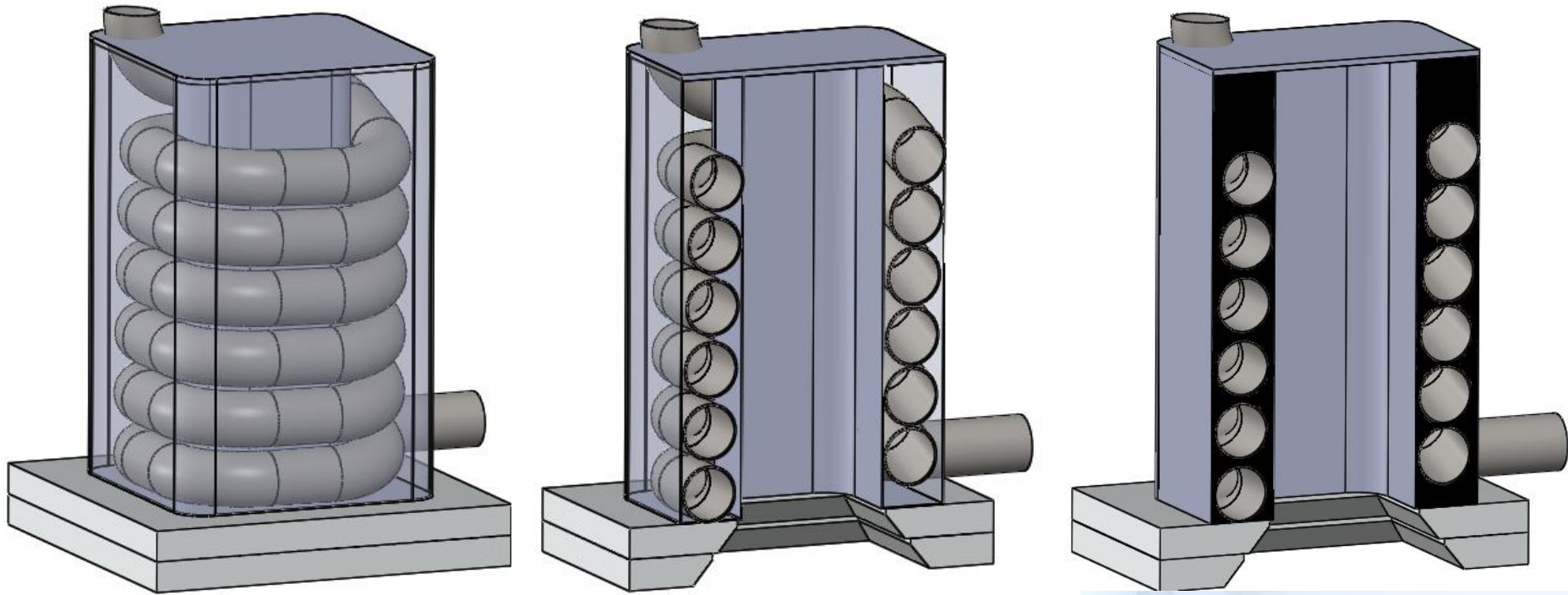


1. Introduction – Open cavity tubular receiver

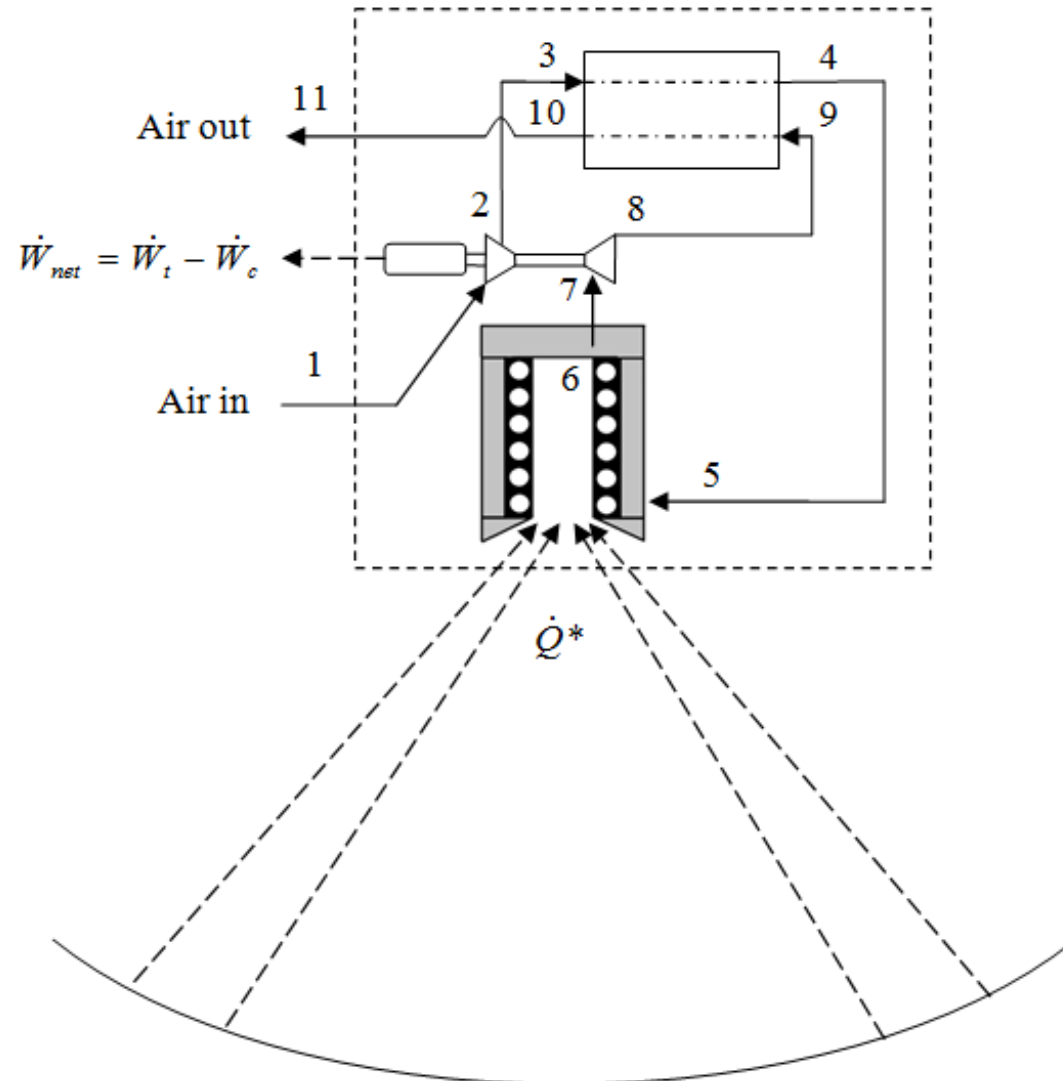
- Heat up insulated receiver to 857 °C
 - using 86 kW LPG flame from Sievert burner



1. Introduction – Brayton cycle thermal storage



1. Introduction – Brayton cycle thermal storage



1. Introduction

Thermal storage

- Lithium fluoride (Cameron et al., 1972; Asselman, 1976)
- Packed rock beds (Allen, 2010; Ozturk et al., 2019),
- Encapsulated sodium sulphate (Klein, 2016)

- **Phase-change materials** can be used to provide a stable turbine inlet temperature;
 - however, most phase-change materials have a **low thermal conductivity** of around 0.5 W/mK (Liu et al., 2012).
 - **metallic phase-change materials** have higher thermal conductivities.
 - Other materials such as salt composites and inorganic salts have limited applications because of large volume changes during melting as well as **corrosion issues** (Liu et al., 2012).

1. Introduction (Solar-dish Brayton cycle)

– Metallic phase-change materials (Liu et al. 2012)

Phase-change material	Composition (wt%)	Melting temperature (K)	ρ (kg/m ³)	$C_{p,solid}$ (J/kgK)	$C_{p,liquid}$ (J/kgK)	k (W/mK)	Latent heat, L_f (kJ/kg)
Mg		921	1740	1270	1370		365
Al		933	2700	900	1100	186	397
Zn–Cu–Mg	49/45/6	976	8670	420			176
Cu–P	91/9	988	5600				134
Cu–Zn–P	69/17/14	993	7000				368
Cu–Zn–Si	74/19/7	1038	7170				125
Cu–Si–Mg	56/27/17	1043	4150	750			420
Mg–Ca	84/16	1063	1380				272
Mg–Si–Zn	47/38/15	1073					314
Cu–Si	80/20	1076	6600	500			197
Cu–P–Si	83/10/7	1113	6880				92
Si–Mg–Ca	49/30/21	1138	2250				305
Si–Mg	56/44	1219	1900	790		70	757

2. Problem and Purpose

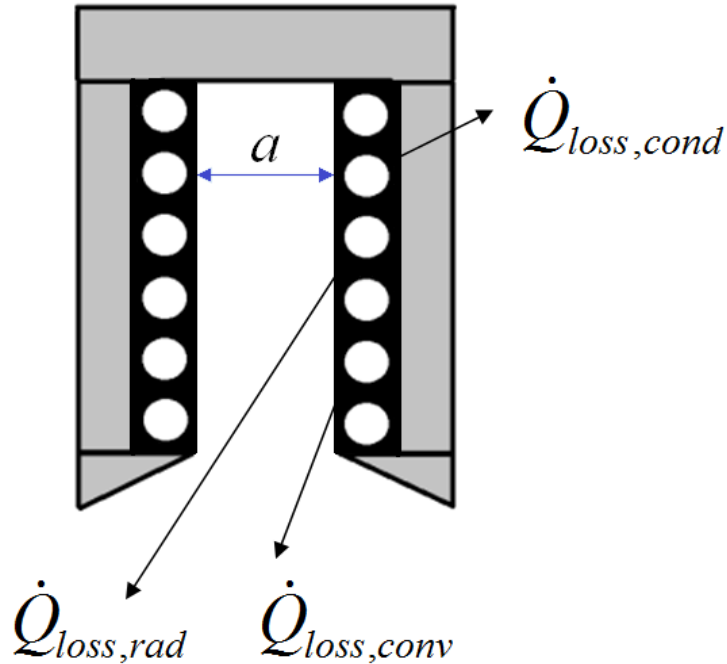
Problem

- the phase-change temperature affects the solar conversion efficiency

Purpose of the study

- Determine maximum thermal efficiency of the cycle for
 - an off-the-shelf turbochargers
 - various recuperator geometries
 - fixed receiver geometry
 - Metallic phase-change material at different solar receiver temperatures

3. Methodology - Receiver



Assumptions for receiver:

- Constant surface temperature tube, at steady state ($T_s = \text{PCM temperature}$)
- Koenig and Marvin heat loss model for cavity receiver

$$T_e = T_s - (T_s - T_i) e^{-h_{rec} A_s / \dot{m} c_p}$$

$$\Delta P = \frac{8 \dot{m}^2}{\rho \pi^2 d^4} \left(f \frac{L}{d} + \sum_y K_y \right)$$

$$\dot{Q}^* = \dot{Q}_{loss,cond} + \dot{Q}_{loss,conv} + \dot{Q}_{loss,rad} + \dot{Q}_{net}$$

$$\dot{Q}_{net} = h_{rec} A_s \frac{(T_i - T_e)}{\ln \left[\frac{(T_s - T_e)}{(T_s - T_i)} \right]}$$

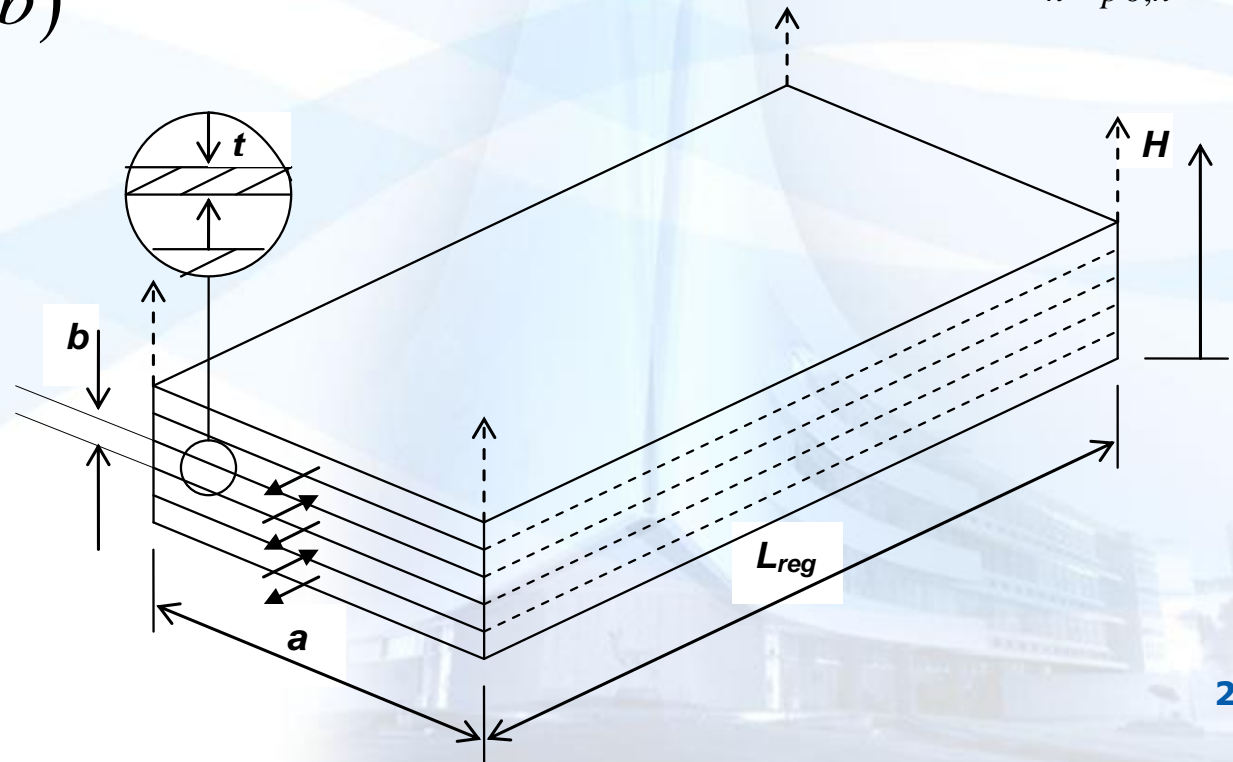
3. Methodology - Recuperator

Assumptions for recuperator:

- Effectiveness-NTU model including heat loss to the environment (Nellis and Pfotenhauer, 2005)

$$\Delta P = \frac{fL_{reg} (\dot{m}/n)^2 (a+b)}{4\rho(ab)^3}$$

$$NTU_h = \frac{UaL_{reg} (2n-1)}{\dot{m}_h c_{p0,h}}$$



3. Methodology - Turbocharger

Assumptions for turbocharger:

- Determine mass flow rate and pressure ratios from the compressor map and turbine map (GT2052)



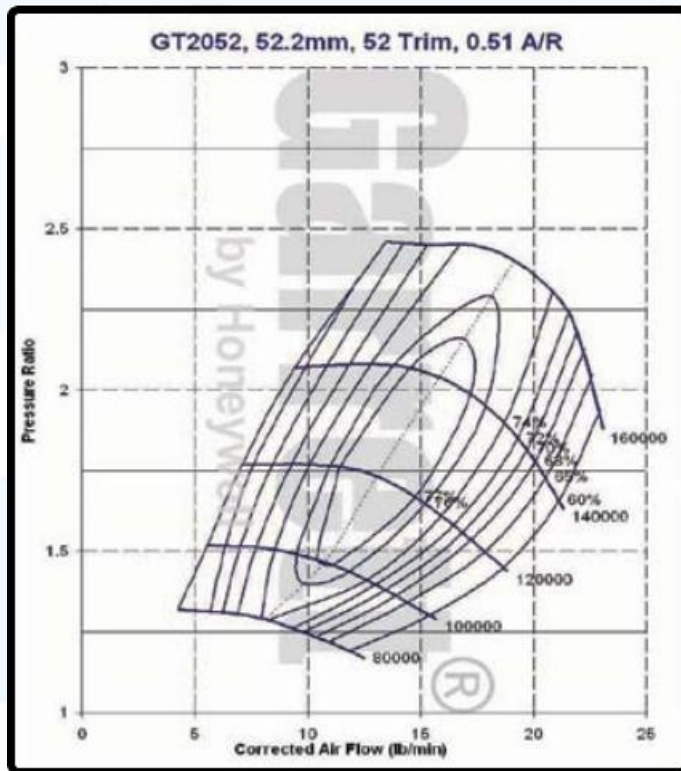
3. Methodology - Turbocharger

Assumptions for turbocharger:

- Determine mass flow rate and pressure ratios from the compressor map and turbine map

$$BSR = \frac{2\pi N \left(\frac{D_t}{2} \right)}{\left[2h_{in} \left(1 - r_t^{\frac{1-k}{k}} \right) \right]^{1/2}}$$

$$\eta_t = \eta_{t,max} \left(1 - \left(\frac{BSR - 0.6}{0.6} \right)^2 \right)$$



3. Methodology – Parameters

Power output calculation:

The MATLAB program has the following structure:

For $T_s = 900:100:1200$,

For each turbine pressure ratio (r_t) in the operating range of the turbine,

For each recuperator design (625 different combinations),

Find net power output and efficiency of cycle.

3. Methodology – Net power output

Entropy generation minimisation to optimise geometries of components for a common goal

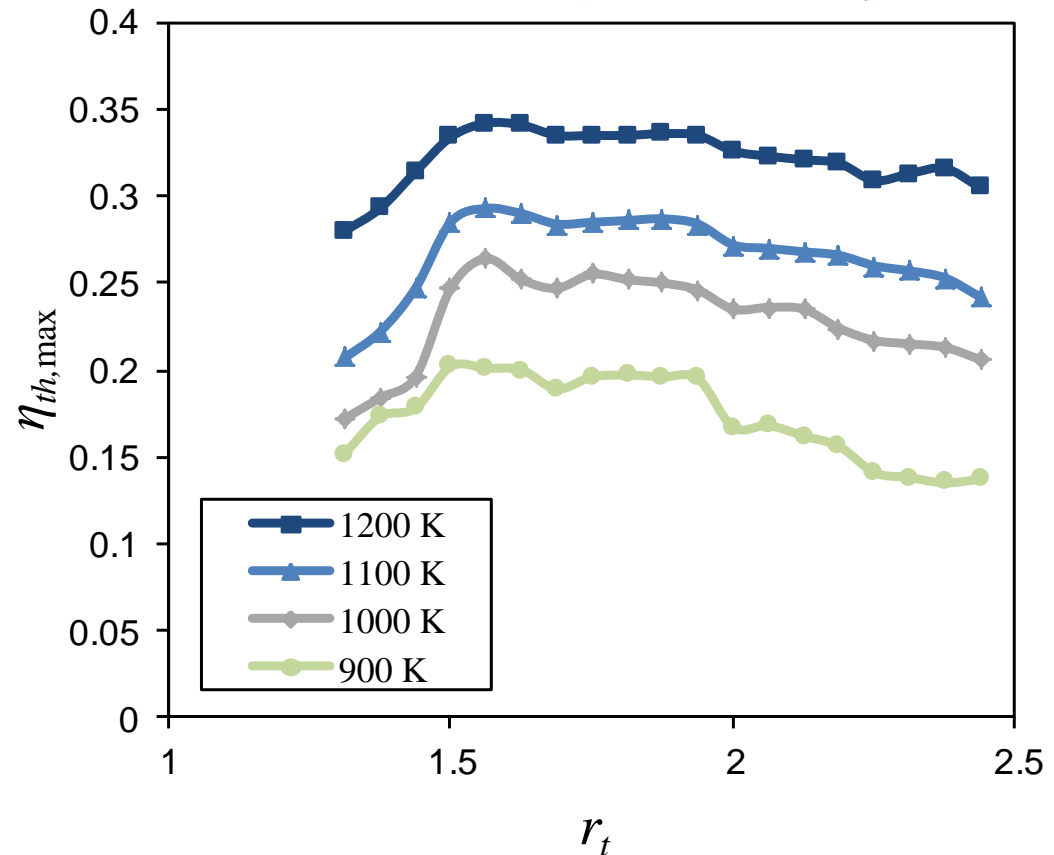
$$\dot{W}_{net} = -T_{\infty} \dot{S}_{gen,int} + \left(1 - \frac{T_{\infty}}{T^*}\right) \dot{Q}^* + \dot{m} c_{p0} (T_1 - T_{11}) - \dot{m} T_{\infty} c_{p0} \ln\left(\frac{T_1}{T_{11}}\right)$$

$$\begin{aligned} \dot{S}_{gen,int} = & \left[-\dot{m} c_{p0} \ln(T_1 / T_2) + \dot{m} R \ln(P_1 / P_2) \right]_{compressor} \\ & + \left[\dot{m} c_{p0} \ln \left[\frac{T_{10} T_4}{T_9 T_3} \left(\frac{P_{10} P_4}{P_9 P_3} \right)^{-R/c_{p0}} \right] + \dot{Q}_{loss,reg} / T_{\infty} \right]_{recuperator} \\ & + \left[-\frac{\dot{Q}^*}{T^*} + \frac{\dot{Q}_{loss}}{T_{\infty}} + \dot{m} c_{p0} \ln(T_6 / T_5) - \dot{m} R \ln(P_6 / P_5) \right]_{receiver} \\ & + \left[-\dot{m} c_{p0} \ln(T_7 / T_8) + \dot{m} R \ln(P_7 / P_8) \right]_{turbine} \end{aligned}$$



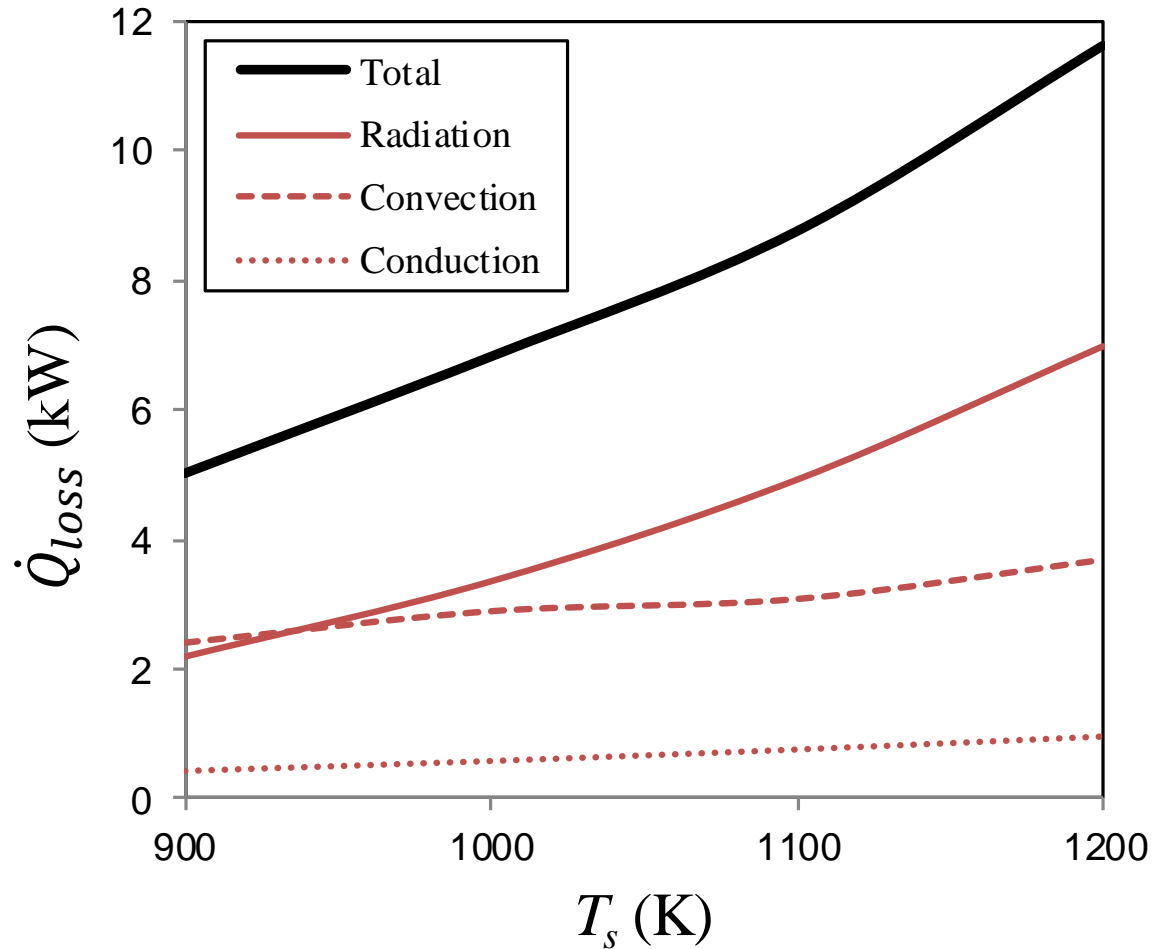
4. Results and discussion- thermal efficiency

Maximum thermal efficiencies of 20.2% to 34.2%



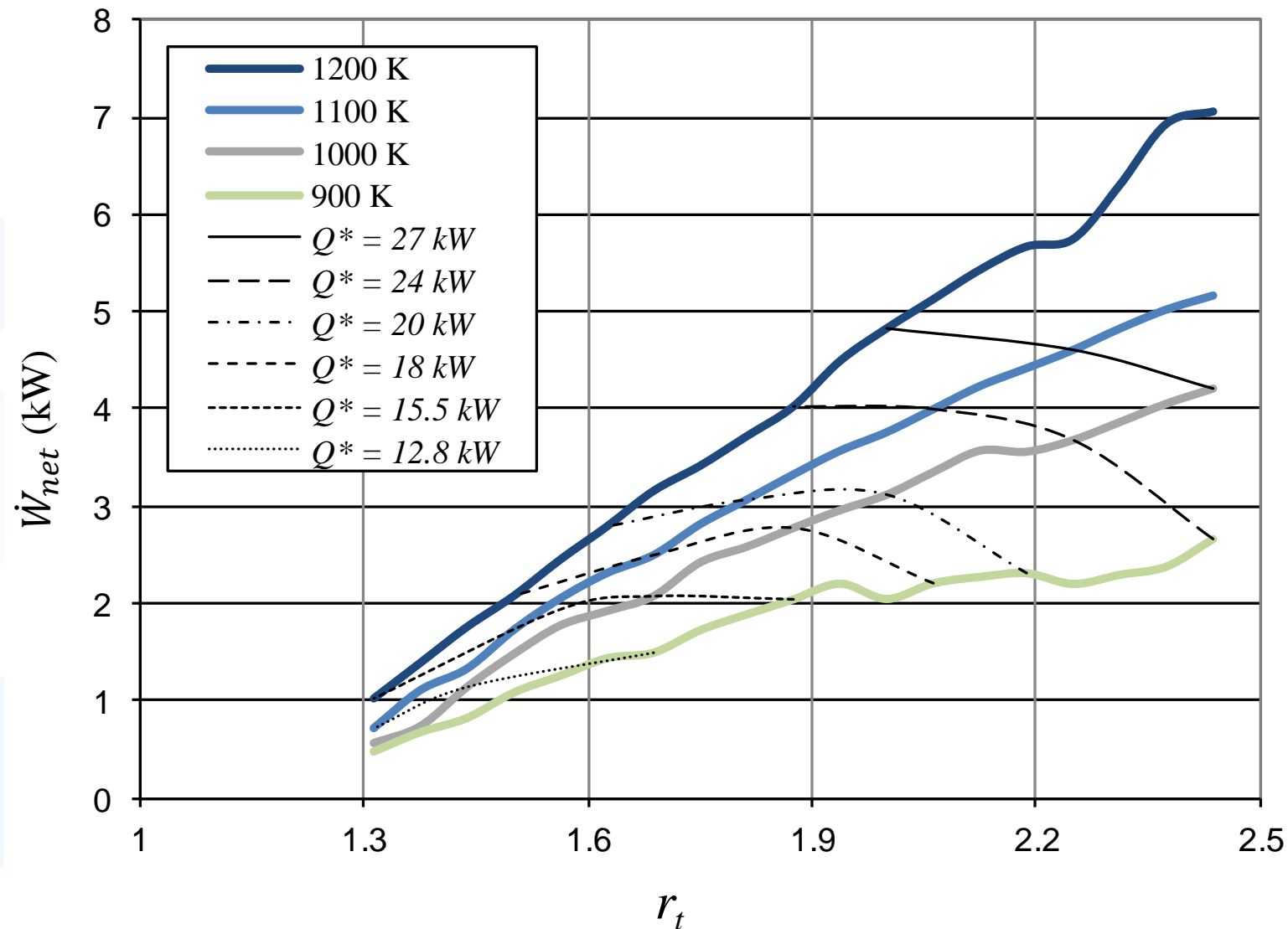
Maximum thermal efficiency of the cycle for different turbine pressure ratios and receiver tube surface temperatures (for *GT2052*).

4. Results and discussion – receiver heat loss



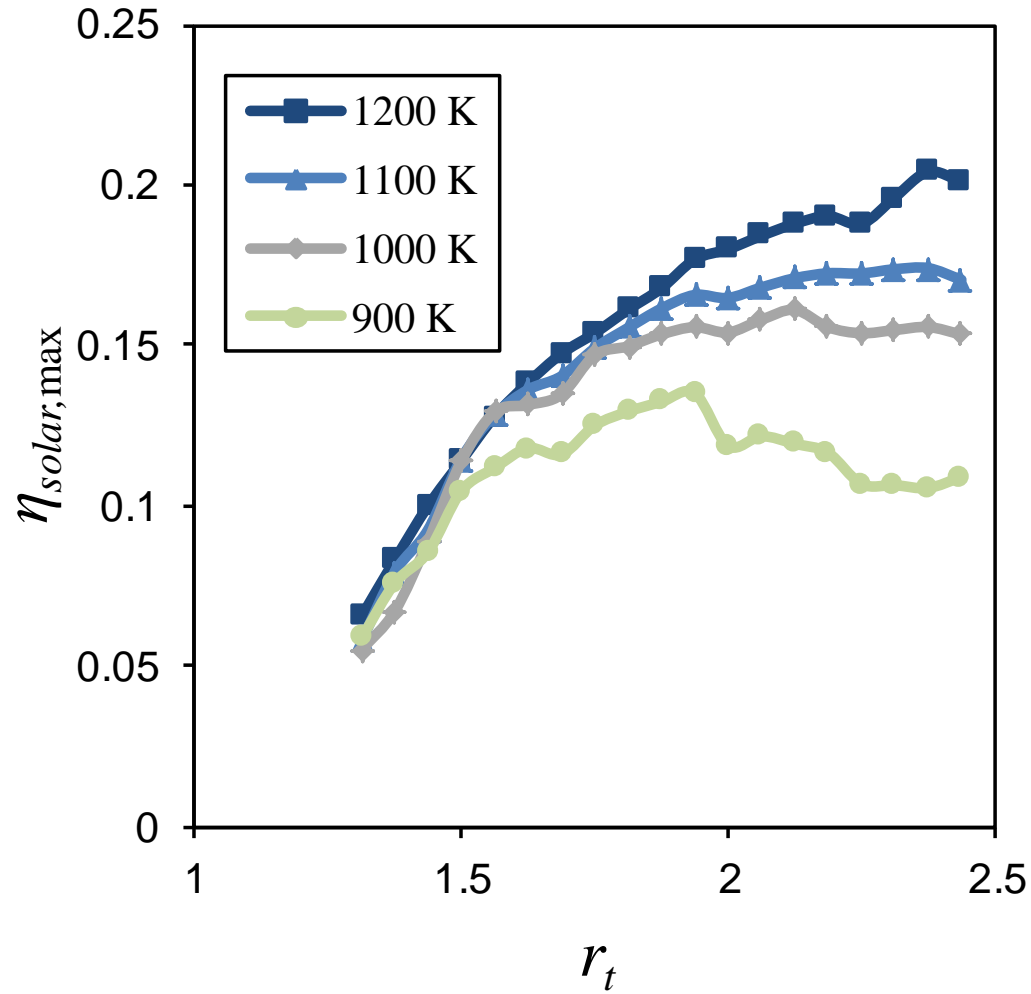
Heat loss rate from the solar receiver as a function of tube surface temperature.

4. Results and discussion – performance map



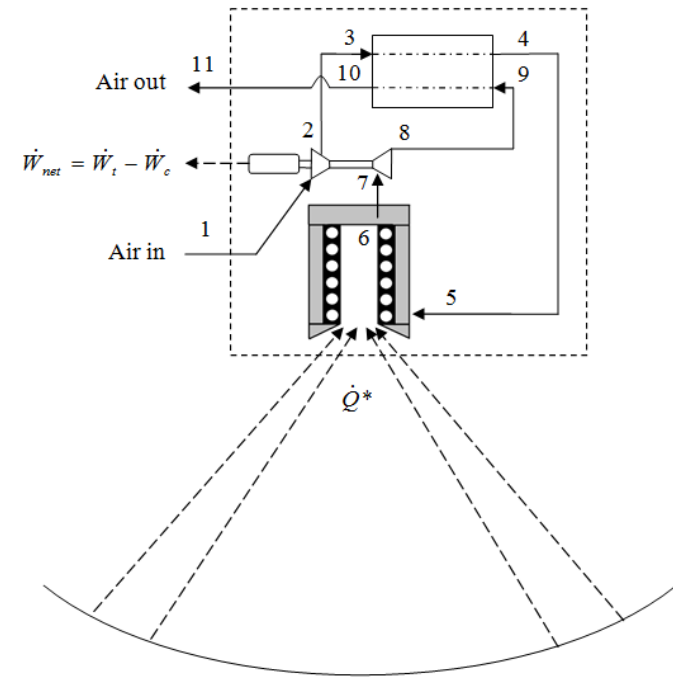
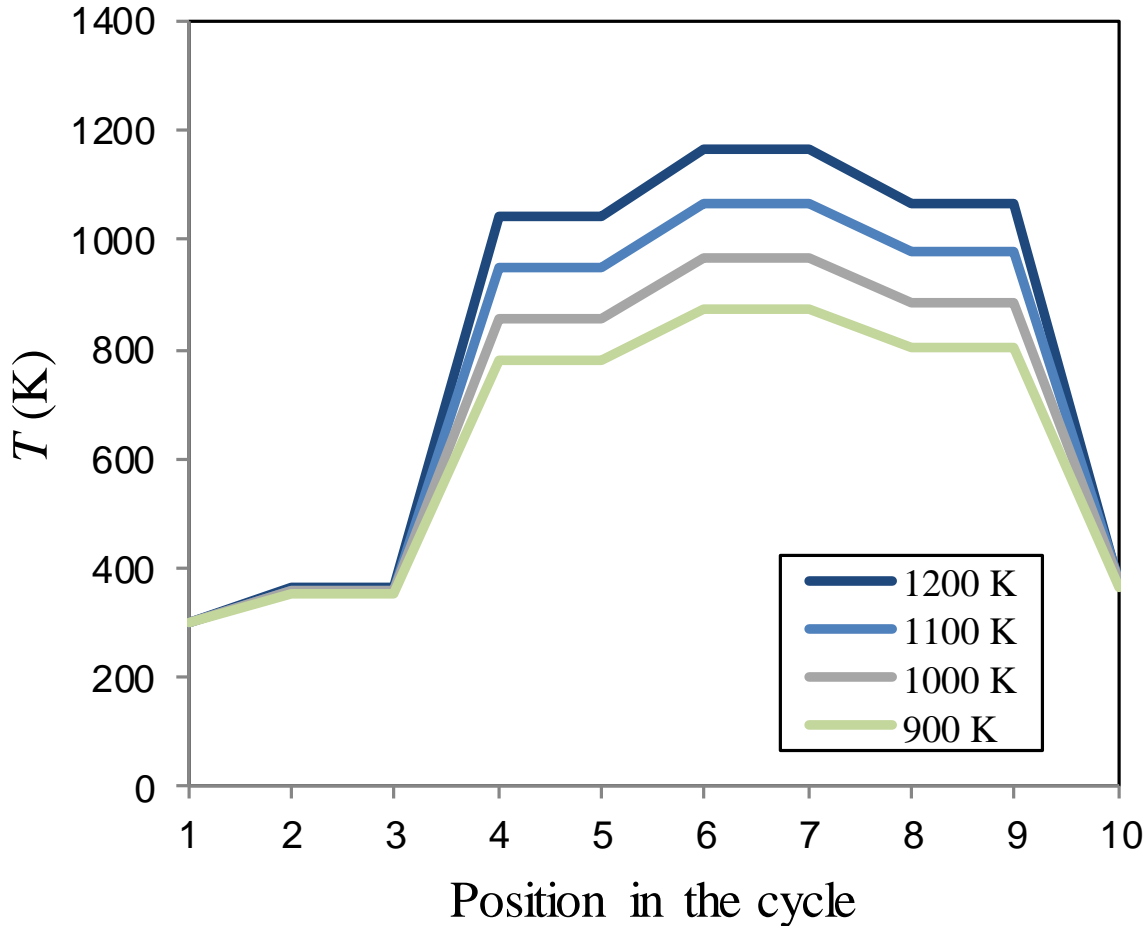
Net power output at maximum thermal efficiency for GT2052 as a function of dish size

4. Results and discussion – solar conversion efficiency



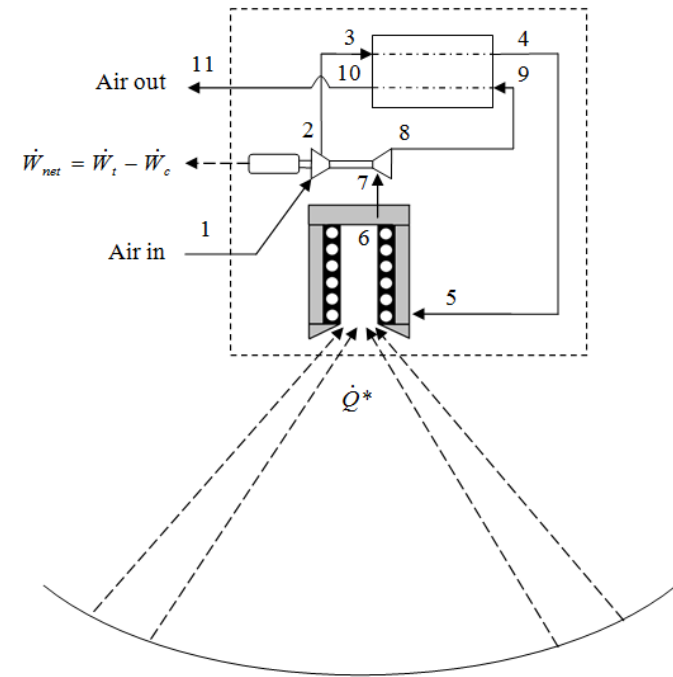
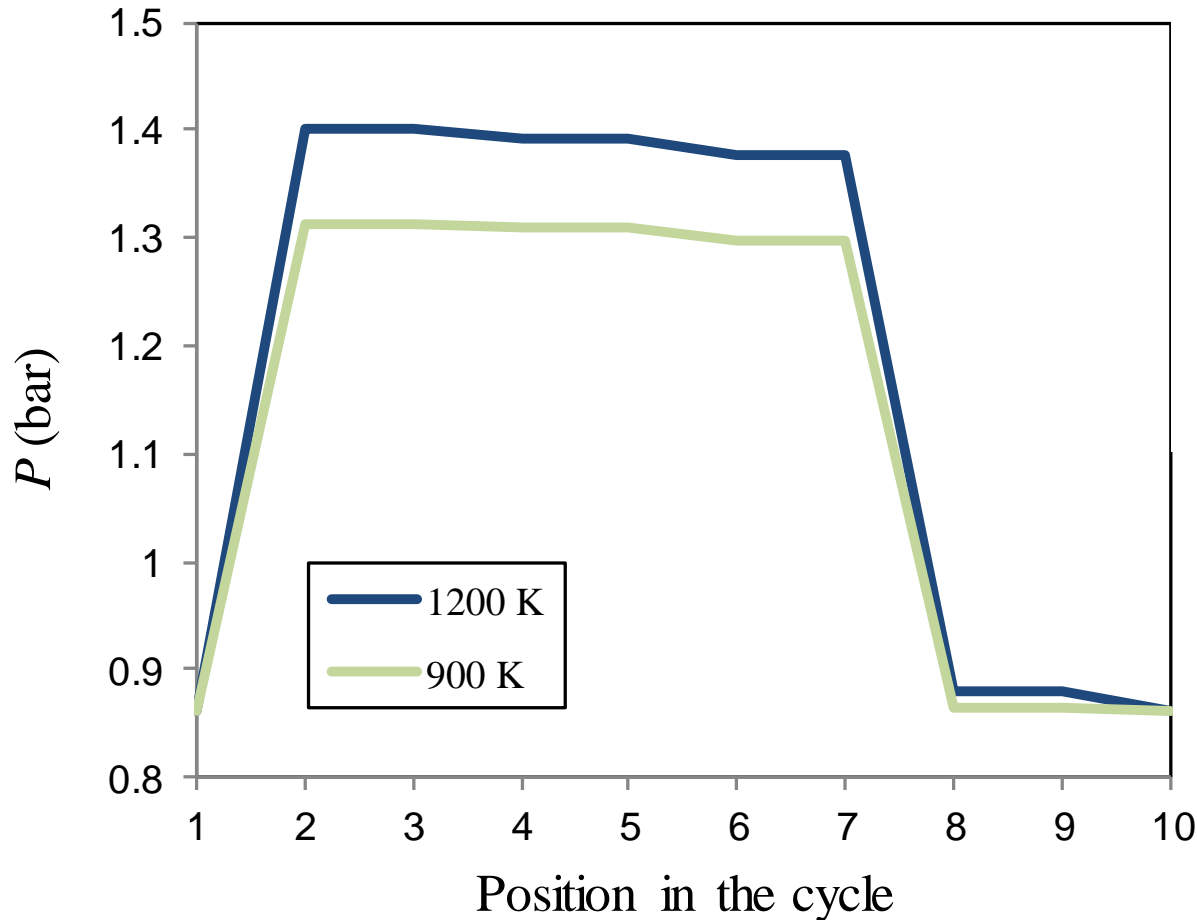
Maximum solar conversion efficiencies of **13.5% to 21%** can be achieved at receiver temperatures of between 900 K and 1200 K.

4. Results and discussion



Temperature in the cycle at different receiver surface temperatures for maximum thermal efficiency (for *GT2052*).

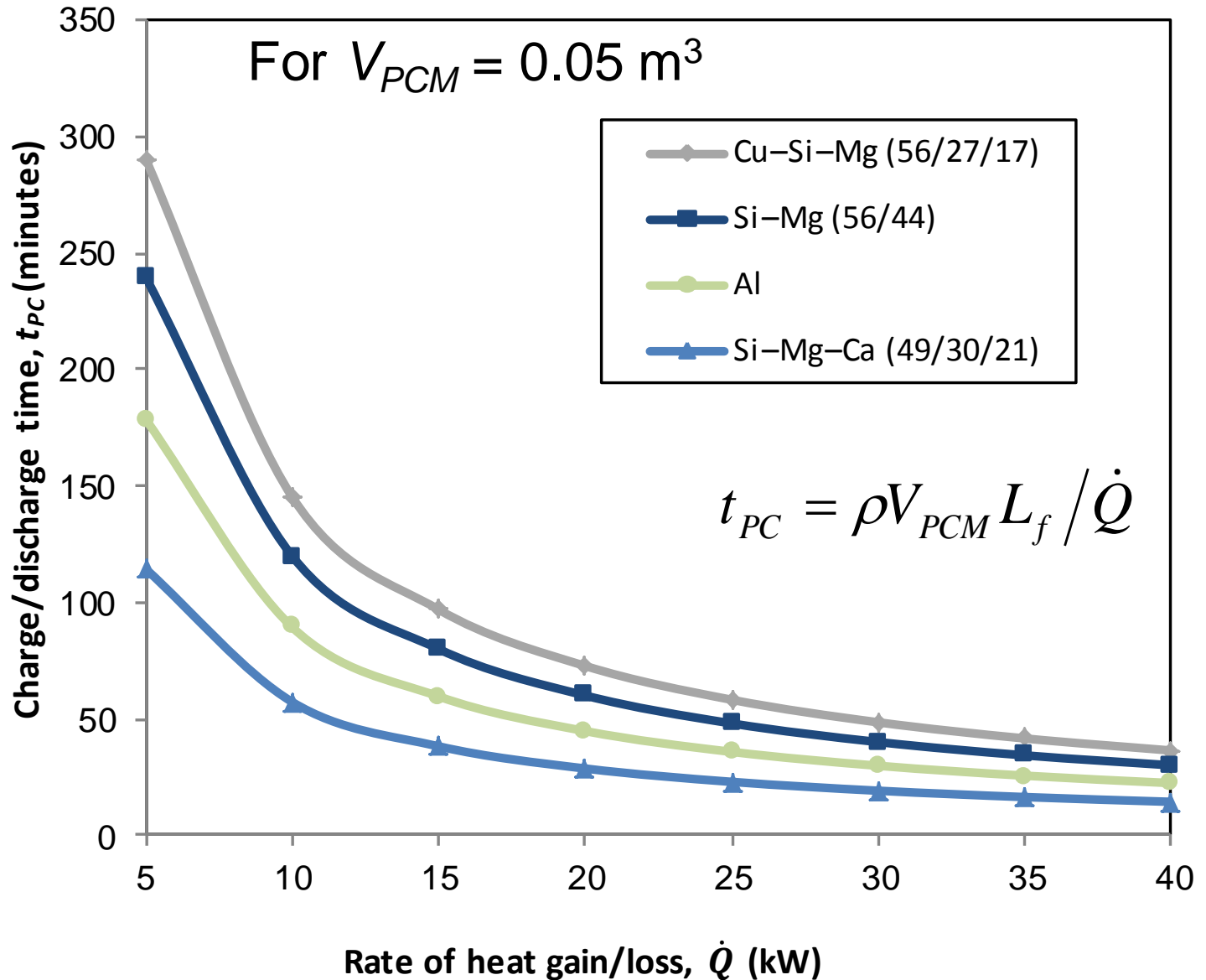
4. Results and discussion



Pressure in the cycle at different receiver surface temperatures for maximum thermal efficiency (for *GT2052*).

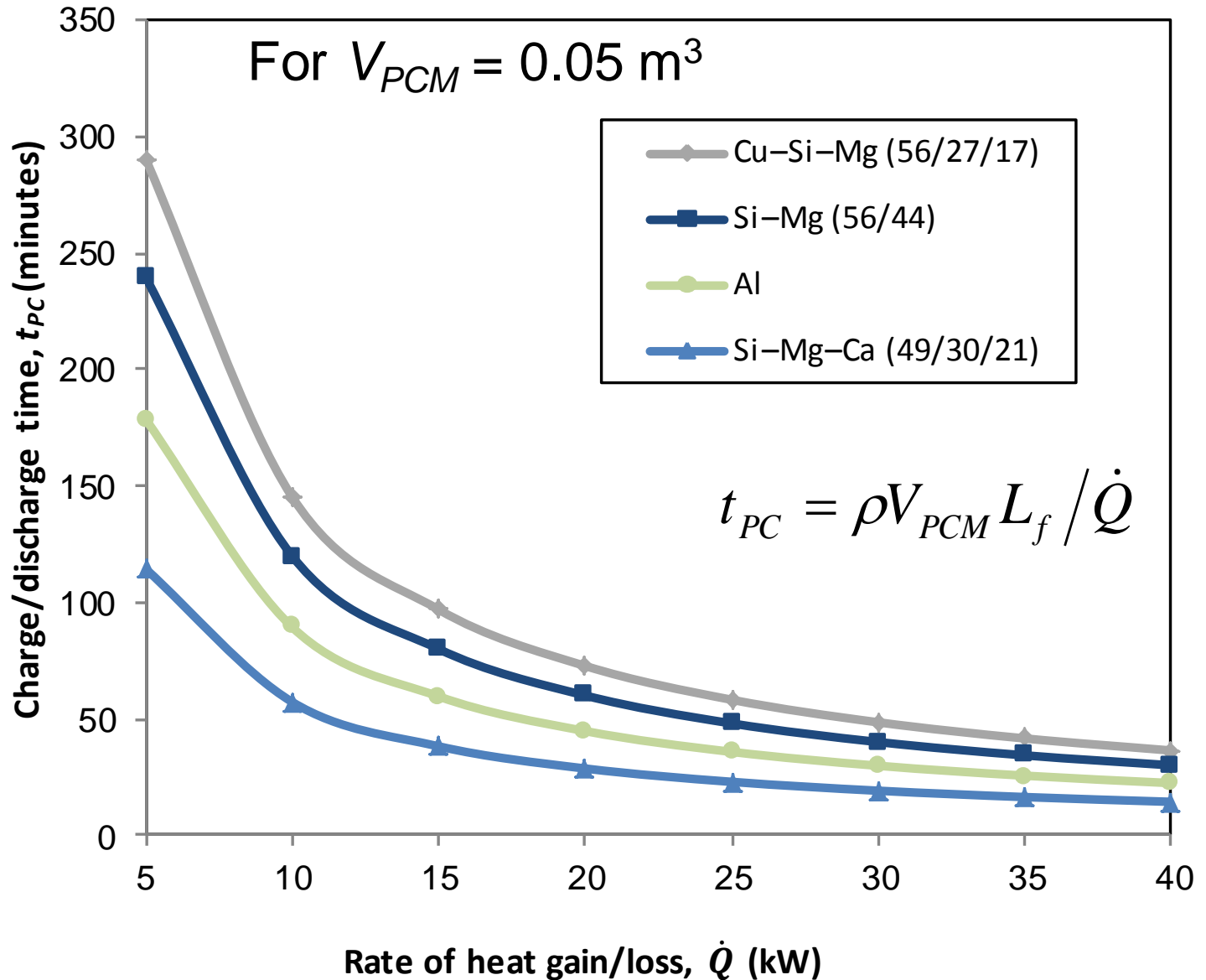
4. Results and discussion – storage time

Thermal storage time available at the phase-change temperature.



4. Results and discussion – storage time

Molten aluminum in the receiver at 933 K, could be worth investigating further as a simple and low-cost solar-dish Brayton cycle configuration.



5. Conclusion

- Solar-dish Brayton cycle advantages:
 - air as working fluid
 - cogeneration
 - hybridisation
 - thermal storage
 - cost benefits, benefits for the economy
- Problem - the phase-change temperature affects the solar conversion efficiency
- Purpose
 - Determine maximum thermal efficiency of the cycle for
 - off-the-shelf turbocharger
 - various recuperator geometries
 - fixed receiver geometry
 - metallic phase-change material at different solar receiver temperatures

5. Conclusion

- **Maximum thermal efficiencies of 20.2% to 34.2%**
- **Maximum solar conversion efficiencies of 13.5% to 21%** can be achieved at **receiver temperatures of between 900 K and 1200 K.**
- Overall, the results show that an open-cavity tubular solar receiver with metallic phase-change thermal storage material can be used together with an off-the-shelf turbocharger for power generation in a recuperated solar-dish Brayton cycle.
- The *GT2052* operating with molten aluminium in the receiver is recommended for further analytical and experimental investigation.

Solar@UP

Dr WG Le Roux

**TIA funded project:
Building a prototype:
Recuperated solar-
dish Brayton cycle
with turbocharger**



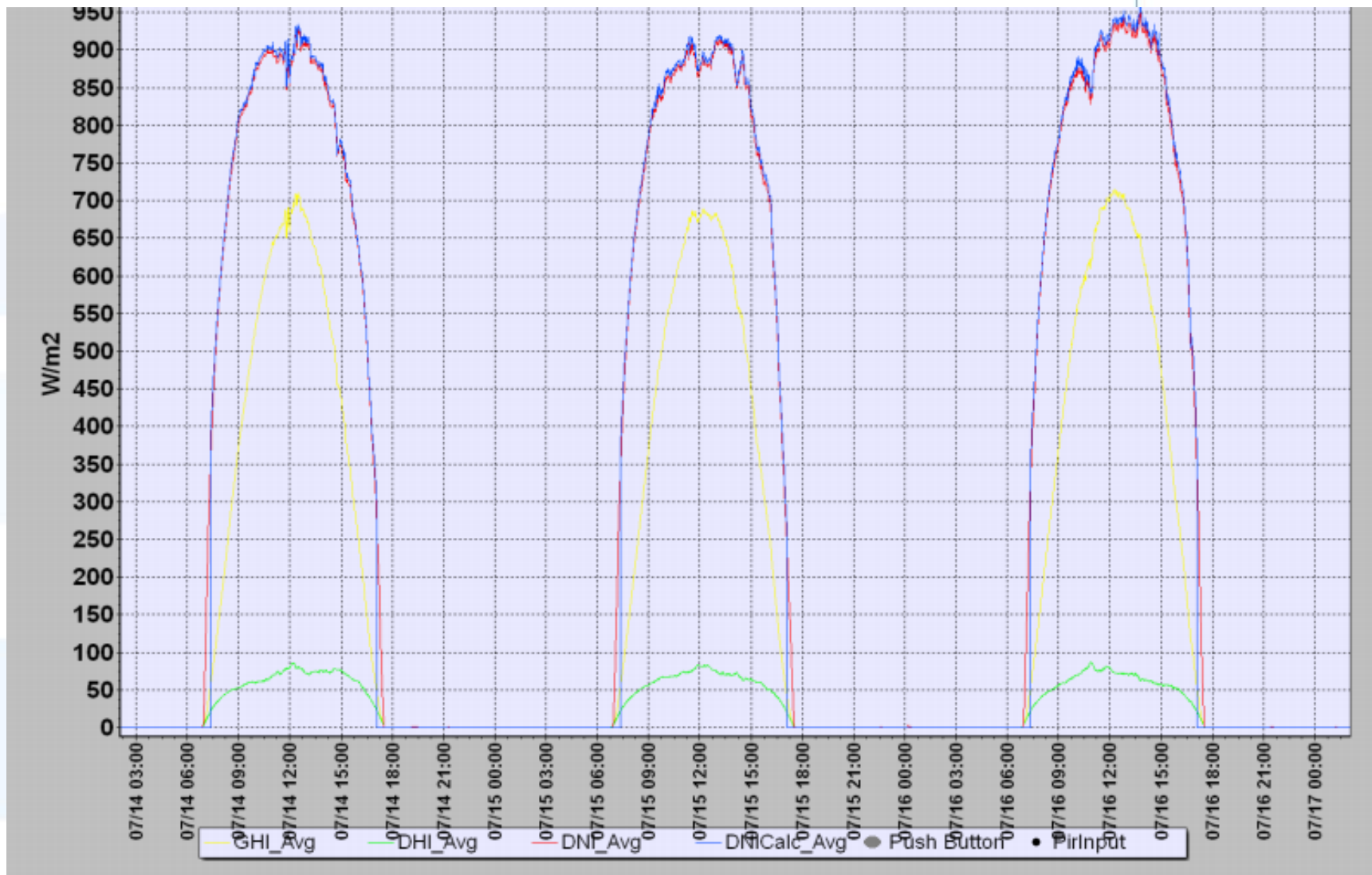
Department of Mechanical and Aeronautical Engineering,
University of Pretoria



UNIVERSITEIT VAN PRETORIA
UNIVERSITY OF PRETORIA
YUNIBESITHI YA PRETORIA

Denkleiers • Leading Minds • Dikgopolo tša Dihlalefi

Solar @ UP – Very good DNI (SAURAN)



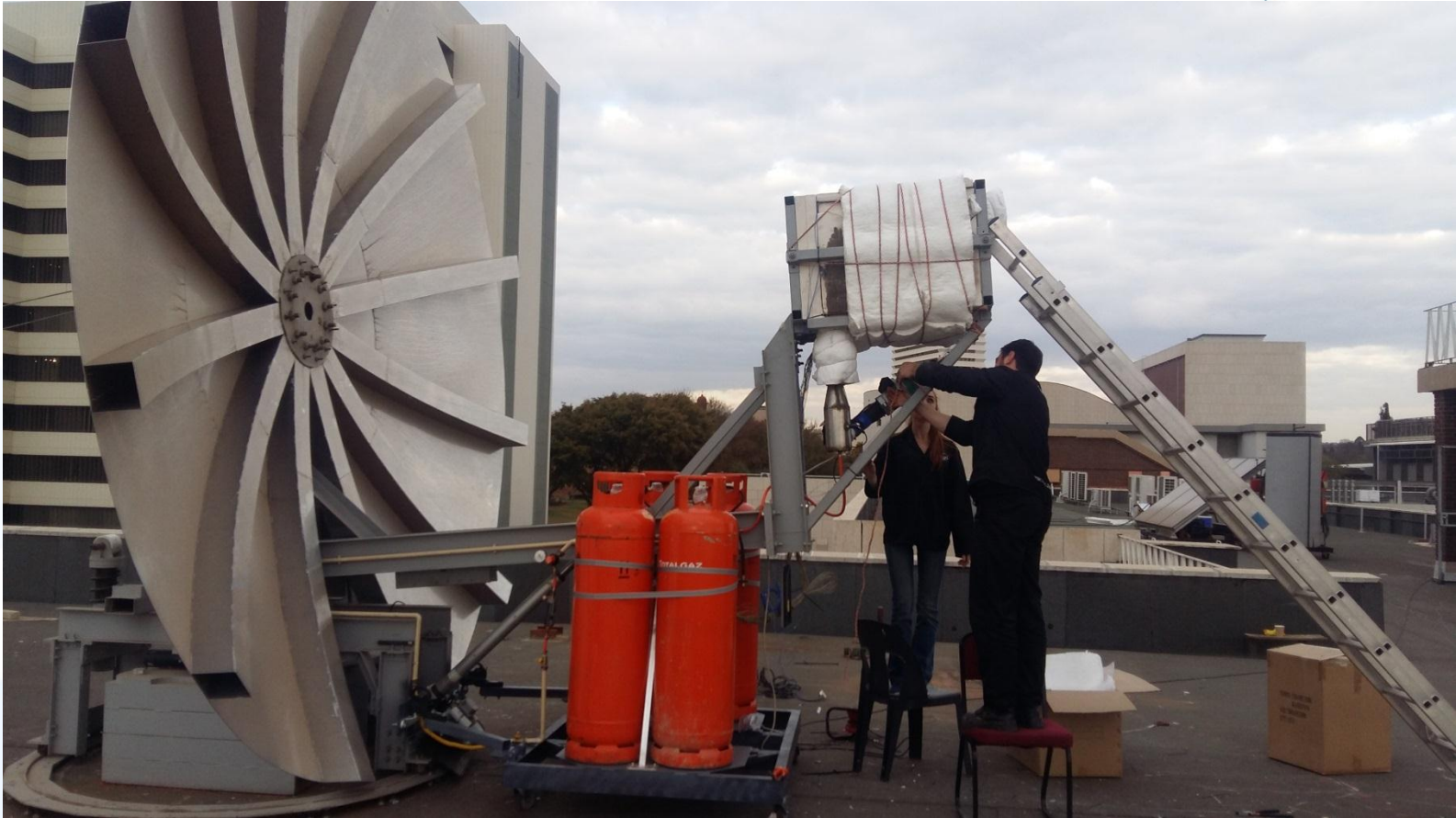
Solar @ UP – old dish



Solar @ UP – old dish



Solar @ UP – old dish



Solar @ UP – Solar receiver testing



Receiver outlet

Insulated receiver

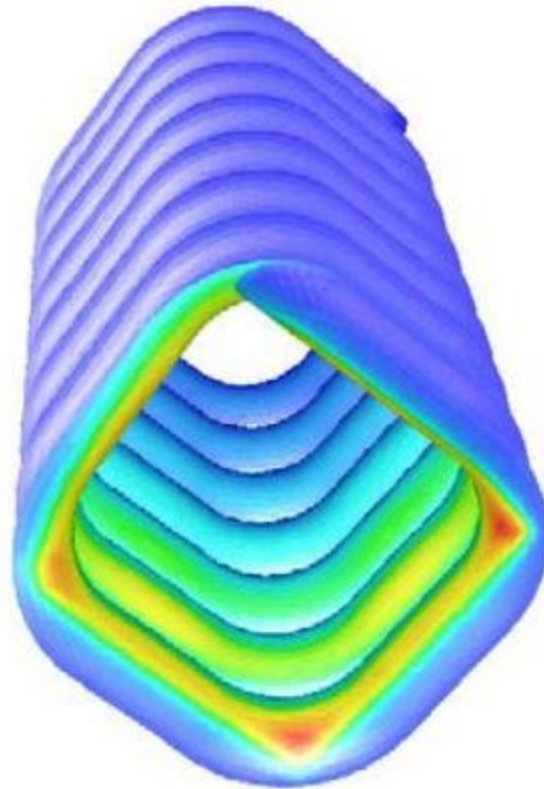
Receiver inlet

Blower and anemometer

Combustion unit



Solar @ UP – CFD (Prof. Ken Craig)



Solar @ UP – new dish



Solar @ UP – new dish



Solar @ UP – new dish



Solar @ UP - new dish



Solar @ UP – new dish



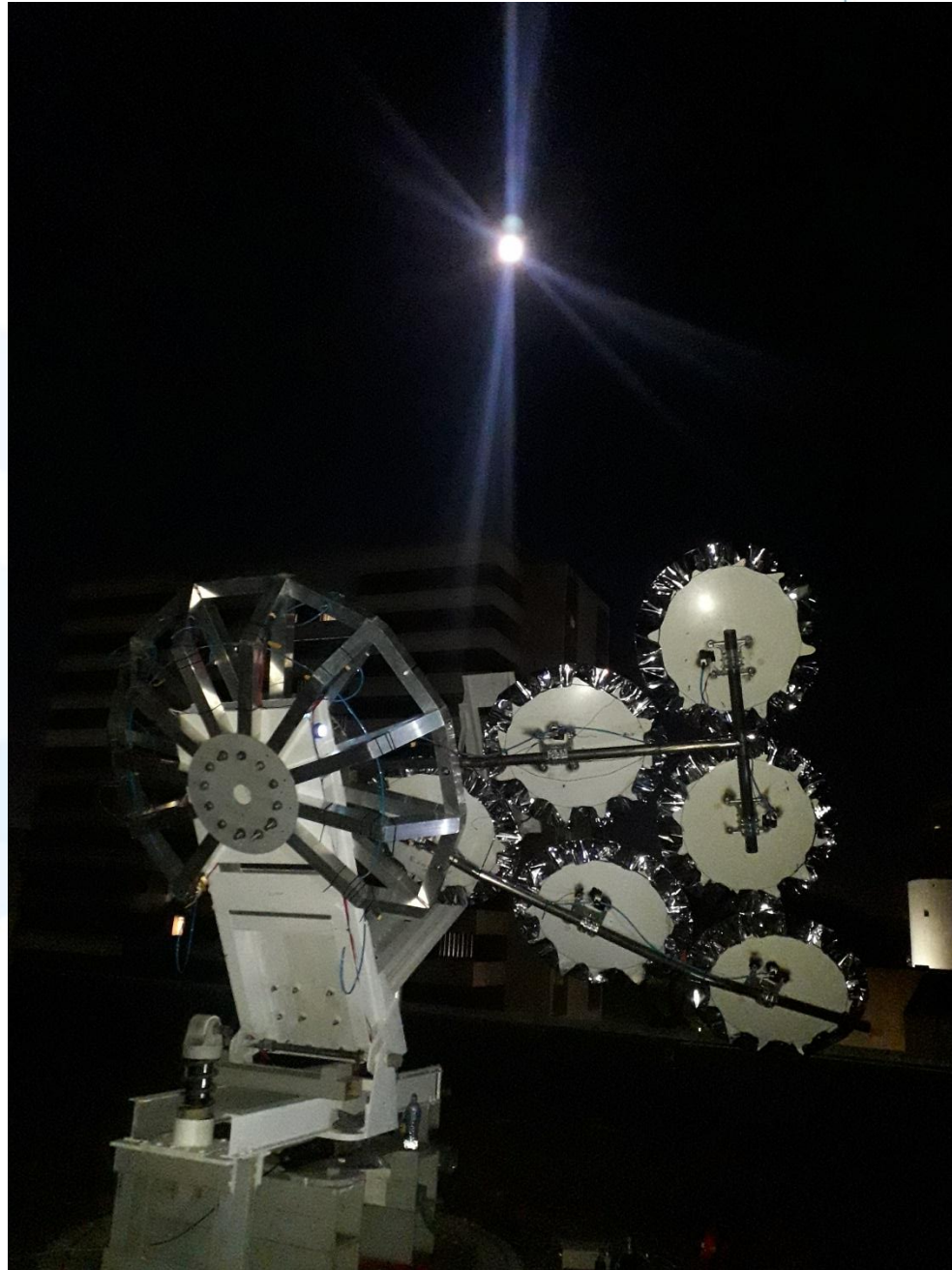
Solar @ UP – new dish (photogrammetry)



Solar @ UP – New dish (Moonlight testing)



Solar @ UP – New dish (Moonlight testing)



Solar @ UP



UNIVERSITEIT VAN PRETORIA
UNIVERSITY OF PRETORIA
YUNIBESITHI YA PRETORIA

Denkleiers • Leading Minds • Dikgopolo tša Dihlalefi

Solar @ UP – New dish (Moonlight testing)



Solar @ UP – New dish (Moonlight testing)



Solar @ UP – New dish (Moonlight testing)



Solar @ UP – Smaller dish setup (moonlight testing)



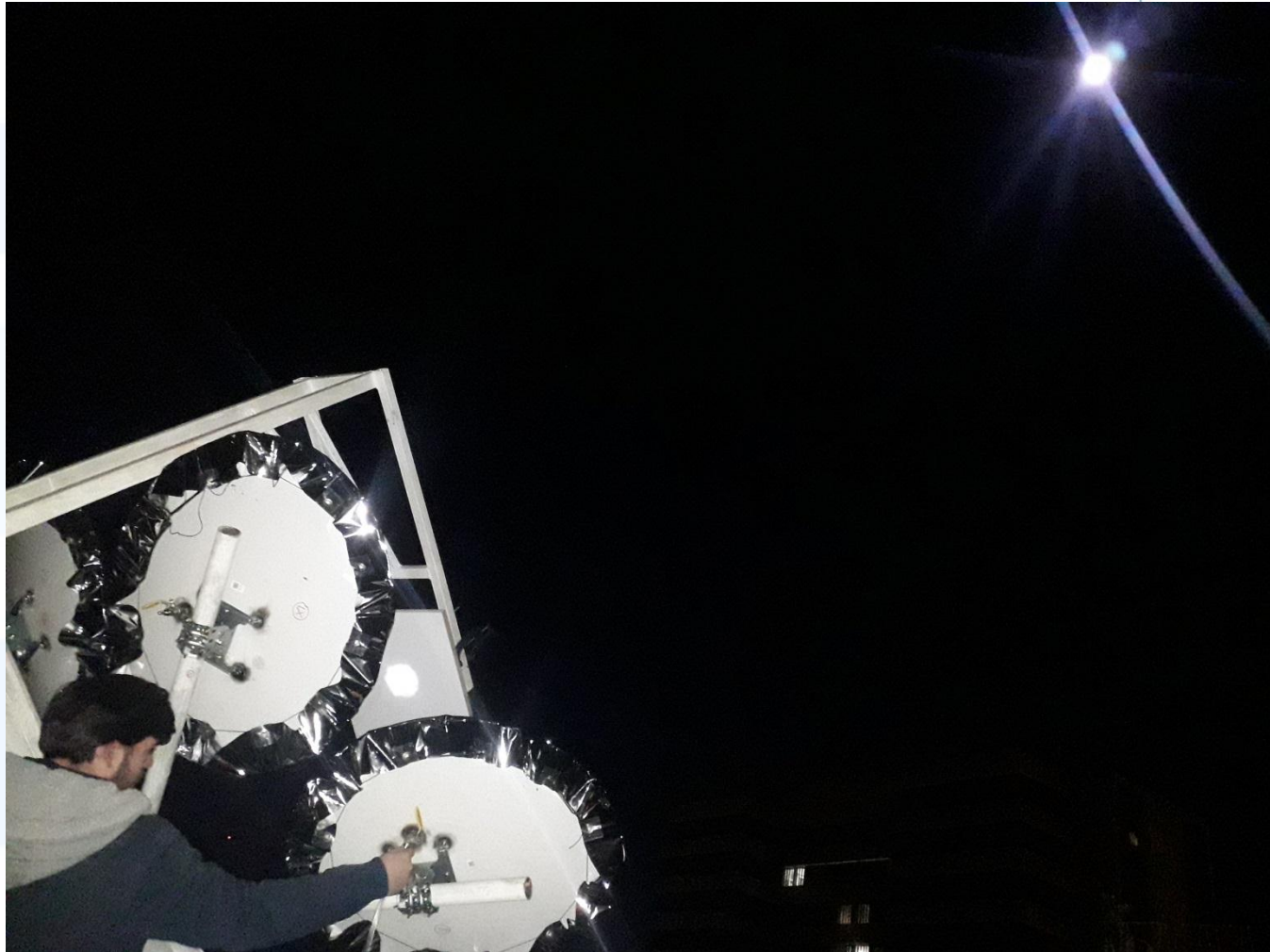
Solar @ UP – Smaller dish setup (moonlight testing)



Solar @ UP – Smaller dish setup (moonlight testing)



Solar @ UP – Smaller dish setup (moonlight testing)



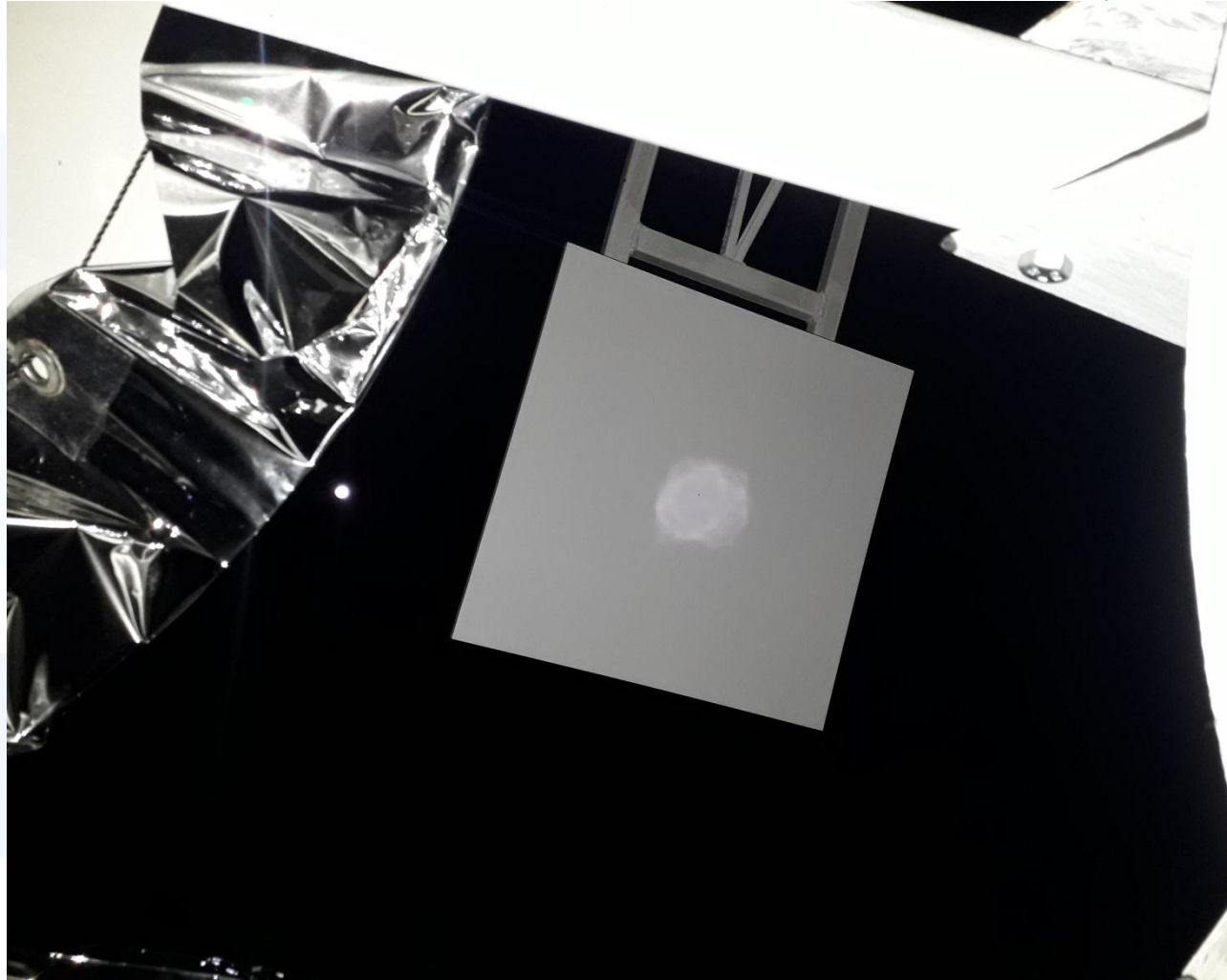
Solar @ UP

– Moonlight testing for flux mapping

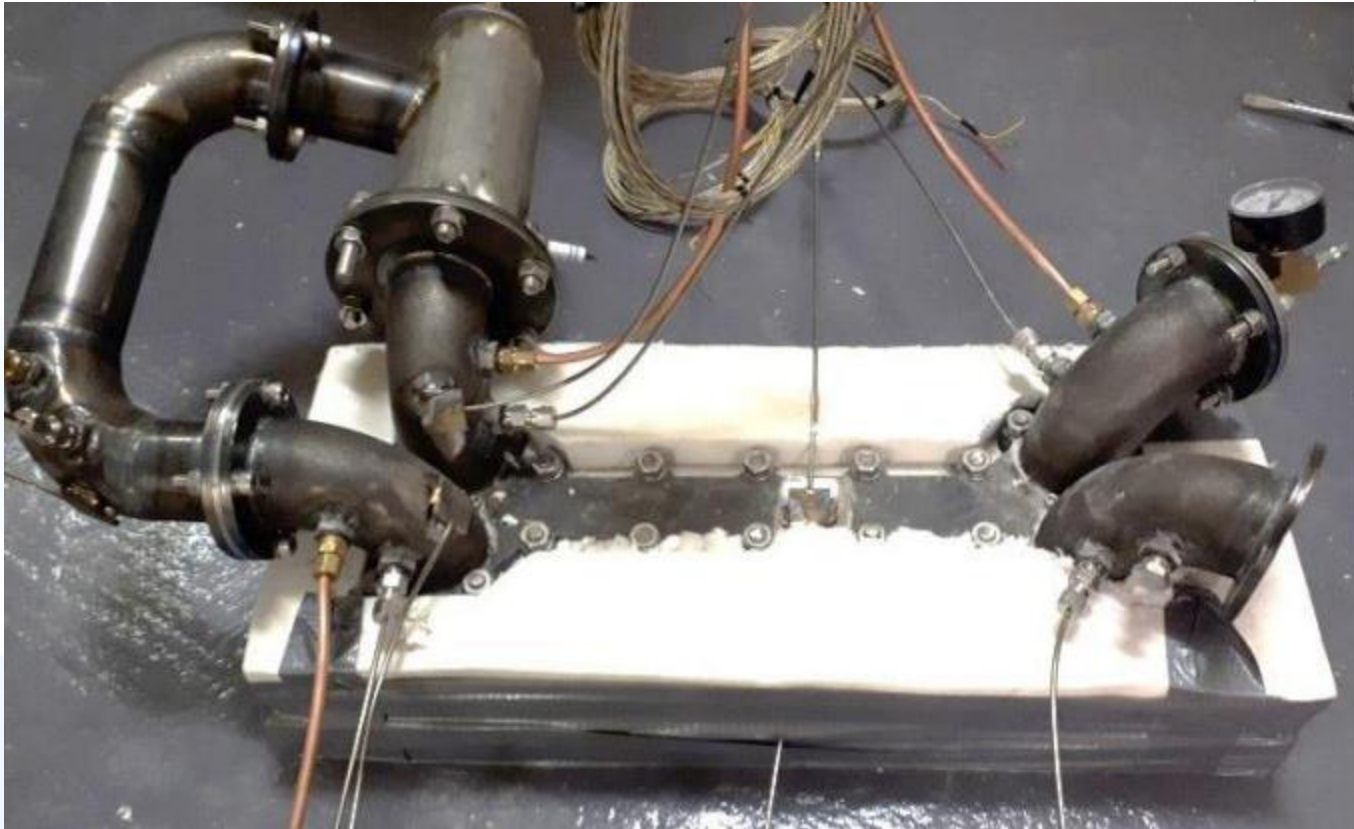


Solar @ UP

– Moonlight testing for flux mapping



Solar @ UP – Recuperator testing



Acknowledgements

- This work is based on the research supported by the
 - **Technology Innovation Agency (TIA),**
 - **National Research Foundation (NRF),**
 - **Royal Society, UK,**
- **SAURAN** is acknowledged for the data used (temperature and wind measurements)

Thank you

Questions?

willem.leroux@up.ac.za

